Thin Film Solvent-Free Photopolymerization of *n*-Butyl Acrylate. I. Static Film Studies

K. V. K. Boodhoo, W. A. E. Dunk, M. S. Jassim, R. J. Jachuck

Process Intensification & Innovation Centre, School of Chemical Engineering and Advanced Materials, University of Newcastle Upon Tyne, Newcastle Upon Tyne NE1 7RU, United Kingdom

Received 20 December 2002; accepted 30 June 2003

ABSTRACT: The results are presented for a detailed investigation involving the free-radical photopolymerization of *n*-butyl acrylate in the form of thin static films. The aim of this work is to benchmark the performance of a novel thin film spinning disk reactor that may be used for the continuous production of linear polymers using photoinitiation. Industrially relevant film thicknesses (200 μm to 1 mm) are studied as opposed to earlier work that looked into extremely thin films (5–25 μm). Such extreme film thicknesses will be difficult to sustain in a thin film reactor without adversely affecting the wettability of the reaction surface and the uniformity of the film. The effects of four main variables (film thickness, UV intensity, initiator concentration, and exposure time) are studied under static film conditions. A 366-nm wavelength is utilized for the UV radiation with 2,2-dimethoxy-2-phenylacetophenone (Irgacure 651) as the photoinitiator dissolved in *n*-butyl acrylate. The molecular weights, polydispersities, and monomer conversions are measured by gel permeation chromatography. In a 400 μm thick film, conversions of >90% can be achieved with an exposure time of 40 s at a radiation intensity of 175 mW/cm^2. The results using the same polymerization system in the spinning disk reactor are presented and compared with the static film results in Part II of this series. J Appl Polym Sci 91: 2079–2095, 2004

Key words: photopolymerization; thin films; poly(butyl acrylate); kinetics; modeling

INTRODUCTION

Esters of acrylic and methacrylic acid are important industrial commodities, and their polymerization is widely practiced and gives a range of homo- and copolymers that have important applications in many areas (e.g., adhesives, coatings, and polishes).[1] These monomers are characterized by having very rapid rates of polymerization and high heats of polymerization, particularly in the case of the lower alkyl acrylates; thus, they are polymerized by solution, emulsion, or suspension techniques.[2] However, these procedures demand the use of solvents, emulsifiers, and suspension stabilizers, the last two being difficult to remove from the polymer. The increasing awareness of adverse environmental effects resulting from indiscriminate use of solvents is the impetus to search for cleaner methods. Bulk polymerization is an excellent candidate because only a monomer and an initiator are needed, and sometimes chain transfer agents for molecular weight control. Unfortunately, the application of the bulk method to industrial-scale polymer production is severely restricted by the strongly exothermic nature of most commercially important monomers and the autoacceleration effect brought about by the prevention of termination reactions as the viscosity increases with the monomer conversion. This effect is particularly enhanced when acrylates are involved, because of the formation of branched structures and insoluble networks at <10% conversion.[1] Acrylates are most often used as comonomers in copolymerization with methacrylates or styrene. However, to avoid highly sheared thin films and micromixing effects on the copolymerization, we decided to work with *n*-butyl acrylate homopolymer. A further consideration is economic because, according to a very recent analysis, *n*-butyl acrylate accounts for 51% of the bulk acrylate demand.[3]

The selection of photoinitiation was the result of several considerations:

1. There is effectiveness over a very wide temperature range. Ambient temperature polymerization would reduce transfer effects and subzero polymerization would favor syndiotacticity in the polymer.[4]
2. There should be zero-activation energy for radical formation; hence, the temperature has little effect on the rate of polymerization. Further, the dissociation of the initiator would be at constant rate, independent of the temperature.

Correspondence to: K. V. K. Boodhoo (k.v.k.boodhoo@ncl.ac.uk).

Contract grant sponsor: Engineering and Physical Sciences Research Council (U.K.); Contract grant number: GR/M73705/01.

3. It provides facile control of free-radical generation.
4. A rapid rate of initiation should be easily achieved and, when comparable to the propagation rate, the polymer polydispersity should be low.

Since the pioneering work on photopolymerization of vinyl and acrylic monomers by Melville and coworkers[5,6] in the 1950s, there has been little published work in this area other than its application to kinetic studies. Utilization of photopolymerization for synthesis of polymers has been the subject of a few patents,[7,8] but none have come to industrial reality. Manga et al. recently reported their work on the use of photoiniferters to achieve controlled free-radical polymerization of *n*-butyl acrylate,[9] but they used toluene as a solvent and worked in Pyrex tubes. By comparison, we use the bulk monomer as a thin static film and achieve similar polydispersities (~2.0) in greatly reduced reaction times (seconds compared to 10s of minutes).

A major part of this investigation is the study of static films with industrially relevant film thicknesses that would allow the development of novel reactor technology for continuous production of polymer resins. Previous investigations have largely concentrated on photocuring applications and the study of the formation of crosslinked polymers in extremely thin films (5–25 μm).[10] In order to understand the photopolymerization of thin films, a brief description of the reaction steps is presented in this study. A theoretical kinetic model of the photopolymerization is also developed and the theoretical conversions based on the model are compared with experimental data obtained under various operating conditions. Finally, we derive empirical models for the photopolymerization of *n*-butyl acrylate, which are particularly suitable for thicker films in the range of 200–1000 μm.

THEORETICAL

Kinetics of photopolymerization reaction

Mechanistic steps

The elementary steps involved in photopolymerization following a free-radical mechanism have been extensively documented in a number of polymer textbooks.[11,12] In brief, these steps are contained in eqs. (1a)–(4c). The first step is the initiator dissociation:

$$I \xrightarrow{h\nu} 2R^{\bullet} \tag{1a}$$

In the case of 2,2-dimethoxy-2-phenylacetophenone (DMPA),

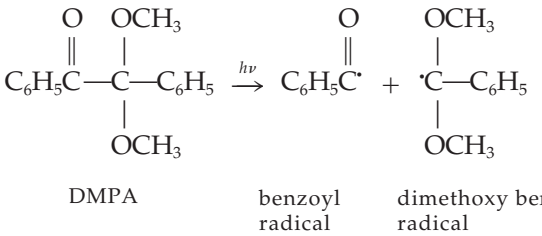

(1b)

where the benzoyl radical is often the major initiating species.[13] The reaction of a primary radical with a monomer proceeds as

$$R^{\bullet} + M \xrightarrow{k_i} RM^{\bullet} \tag{2}$$

The propagation by monomer addition is

$$RM^{\bullet} + M \xrightarrow{k_p} RM_2^{\bullet} \tag{3a}$$

$$RM_n^{\bullet} + M \xrightarrow{k_p} RM_{n+1}^{\bullet} \tag{3b}$$

Termination of active chains is by combination,

$$RM_x^{\bullet} + RM_y^{\bullet} \xrightarrow{k_{tc}} RM_{x+y}R \tag{4a}$$

or disproportionation,

$$RM_x^{\bullet} + RM_y^{\bullet} \xrightarrow{k_{td}} RM_p + RM_q \tag{4b}$$

Under certain conditions (e.g., high concentrations of primary radicals and low monomer concentrations, etc.) the termination of an active chain may occur by a primary radical:

$$RM_x^{\bullet} + R^{\bullet} \xrightarrow{k_{tc}} RM_xR \tag{4c}$$

Rate expressions

Initiation. In the simplest case, the local rate of initiation R_i, [eq. (2)] is dictated by the rate of dissociation of the initiator by UV irradiation [eq. (1)]:

$$R_i = R_d = 2\phi_i I_a \tag{5}$$

where ϕ_i is the quantum yield of initiation and I_a is the volumetric photon absorption rate (mol/L s).

Assuming that the Beer–Lambert law is applicable, the average absorbed light intensity across the thickness (l) of the film is given by

$$\bar{I}_a = I_o(1 - e^{-\alpha lC}) \tag{6}$$

where I_o is the incident light intensity [mol/(1000 s cm^2) or einsteins/1000 s cm^2], α is the absorption coefficient (L mol^{-1} cm^{-1}), l is the pathlength or film thickness (cm), and C is the concentration of light absorbing species in the film (mol/L).

When using a nonphotobleaching initiator such as DMPA, all photoinitiator moieties (initiator molecules, initiator free radicals, and end groups in the polymer molecules) that absorb light have to be considered. Hence, C represents the concentration of all photoinitiator moieties involved and not the concentration of the initiator itself. If the various absorbing species have different absorption coefficients, then the exponential term in eq. (6) will be of the form $\alpha_1 lC_1 + \alpha_2 lC_2 + \cdots$; but, for simplification purposes, it is fairly reasonable to assume that the absorption coefficient is constant for DMPA and all its decomposition products. Thus, we adopt the simplified form of eq. (6).

Note that we adopted the notation α used by Terrones and Pearlstein[14] instead of ϵ for the molar absorption coefficient or extinction coefficient (where $\alpha = \epsilon \ln 10$) to distinguish between the natural log (base e) employed here and the $\log_{10}$ used in the accepted definition of the Beer–Lambert law.[11]

To obtain a volumetric photon absorption rate or a local absorption rate, we differentiate eq. (6) with regard to l.[14–16]

$$I_a = \frac{d\bar{I}_a}{dl} = \alpha C I_o e^{-\alpha lC} \tag{7}$$

Substituting for I_a in eq. (5),

$$R_i = 2\phi_i \alpha C I_o e^{-\alpha lC} \tag{8}$$

The local rate of propagation (R_p), which is also the overall local rate of photopolymerization, follows from the reaction step in eq. (3):

$$R_p = k_p[M][M^\bullet] \tag{9}$$

The local rate of the termination reaction represented by eqs. (4a) and (4b) can be written as

$$R_t = 2k_t[M^\bullet]^2 \tag{10}$$

where k_t is the overall termination rate constant ($k_t = k_{tc} + k_{td}$). For simplicity, the primary termination reactions as expressed in (4c) are assumed to be negligible.

If polymerization takes place under steady-state conditions, $R_i = R_t$ and the local rate of polymerization at a distance l from the film surface becomes

$$R_p = k_p[M]\sqrt{\frac{R_i}{2k_t}} \tag{11}$$

Substituting for R_i from eq. (8) into eq. (11),

$$R_p = k_p[M]\sqrt{\frac{\phi_i \alpha C I_o e^{-\alpha lC}}{k_t}} \tag{12}$$

The measured polymerization rate for any system is the average rate ($\overline{R_p}$) across the film thickness (L) and $\overline{R_p}$ is given by the integral of the local R_p across the thickness of the film (from $l = 0$ to $l = L$) divided by L.[16,17]

$$\bar{R}_p = \frac{1}{L}\int_0^L R_p dl \tag{13}$$

After integration, eq. (13) becomes

$$\bar{R}_p = \frac{2k_p[\bar{M}]}{L}\sqrt{\frac{\phi_i I_o}{\alpha \bar{C} k_t}}(1 - e^{-0.5\alpha L\bar{C}}) \tag{14}$$

In addition, because $\overline{R}_p = -(d[\overline{M}]/dt)$,

$$\int_{[M]_0}^{[\bar{M}]} -\frac{d[\bar{M}]}{[\bar{M}]} = \frac{2k_p}{L}\sqrt{\frac{\phi_i I_0}{\alpha k_t}}\int_0^t \frac{(1 - e^{-0.5\alpha L\bar{C}})}{\sqrt{\bar{C}}}\,dt \tag{15}$$

which gives

$$[\bar{M}] = [M]_0 \exp\left\{-\frac{2k_p}{L}\sqrt{\frac{\phi_i I_o}{\alpha k_t}}\int_0^t \frac{(1 - e^{-0.5\alpha L\bar{C}})}{\sqrt{\bar{C}}}\,dt\right\} \tag{16}$$

where $[\overline{M}]$ is the average monomer concentration in the film (neglecting layer variations) and $\overline{C}$ is the layer-average concentration of light absorbing photoinitiator fragments after time t.

The layer-average monomer conversion after time t is expressed as

$$\bar{X} = 1 - \frac{[\bar{M}]}{[M]_0} \tag{17}$$

Substituting for $[\overline{M}]$ from eq. (16) into (17),

$$\bar{X} = 1 - \exp\left\{-\frac{2k_p}{L}\sqrt{\frac{\phi_i I_0}{\alpha k_t}}\int_0^t \frac{(1 - e^{-0.5\alpha L\bar{C}})}{\sqrt{\bar{C}}}\,dt\right\} \tag{18}$$

Assuming that each DMPA molecule dissociates into two radicals and that the original DMPA molecule and

its radicals are the only absorbing species, the $\bar{C}$ of light absorbing species can be expressed as

$$\bar{C} = [\overline{PI}] + 2([PI]_0 - [\overline{PI}]) \quad (19)$$

where $[PI]_0$ is the initial photoinitiator concentration and $[\overline{PI}]$ is the average photoinitiator concentration after time t. Hence,

$$\bar{C} = 2[PI]_0 - [\overline{PI}] \quad (20)$$

Terrones and Pearlstein[14] stipulated that the rate of decrease of the $[\overline{PI}]$ with time can be expressed as

$$-\frac{d[\overline{PI}]}{dt} = \frac{\phi_i I_o}{L}(1 - e^{-\alpha \bar{C} L}) \quad (21)$$

Oster and Yang[18] used an approximation for eq. (21) in the development of their model for photopolymerization, which has limited applicability to systems with low absorbance (i.e., where $A = \alpha CL$ approaches zero):

$$-\frac{d[\overline{PI}]}{dt} = \phi_i \alpha I_0 \bar{C} \quad (22)$$

[Oster and Yang[18] omitted dividing eq. (21) by L, as was correctly pointed out by Terrones and Pearlstein[14] in their analysis of expressions used for the disappearance of the photoinitiator. Thus, the simplified expression used by Oster and Yang included the L term in their version of eq. (22).[18]]

For simplification purposes, we assume that, because the film thickness used in the current investigation is less than 1 mm and the initial photoinitiator concentration is relatively low (0.0712M), the thin film approximation used by Oster and Yang[18] is applicable to this study. Hence, substituting $\bar{C} = 2[PI]_0 - [\overline{PI}]$ from eq. (20) into eq. (22) gives, on integration,

$$[\overline{PI}] = 2[PI]_0 - [PI]_0 e^{\phi_i \alpha I_0 t} \quad (23)$$

Therefore,

$$\bar{C} = 2[PI]_0 - [\overline{PI}] = [PI]_0 e^{\phi_i \alpha I_0 t} \quad (24)$$

From eq. (20) it is obvious that the $\bar{C}$ will vary initially from $[PI]_0$ (at $t = 0$) to $2[PI]_0$ at a certain maximum time (t_{max}) when all initiator molecules will have dissociated into radical species. The t_{max} when all the initiator molecules have been consumed can be obtained from

$$t_{max} = \frac{\ln 2}{\phi_i \alpha I_0} \quad (25)$$

By substituting $\bar{C}$ from eq. (24) into eq. (14), the $\overline{R_p}$ can be written as

$$\bar{R}_p = \frac{2k_p[\bar{M}]}{L}\sqrt{\frac{\phi_i I_o}{\alpha k_t [PI]_0}} \times [1 - \exp(-0.5\alpha L[PI]_0 e^{\phi_i \alpha I_0 t})] e^{-0.5\phi_i \alpha I_0 t} \quad (26)$$

If a thin film approximation is used, then the term $1 - \exp(-0.5\alpha L[PI]_0 e^{\phi_i \propto I_0 t})$ in eq. (26) can be expanded following Taylor's theorem up to second-order terms of the exponent:

$$[1 - \exp(-0.5\alpha L[PI]_0 e^{\phi_i \alpha I_0 t})] \approx 0.5\alpha L[PI]_0 e^{\phi_i \alpha I_0 t}(1 - 0.25\alpha L[PI]_0 e^{\phi_i \alpha I_0 t}) \quad (27)$$

Then, $\overline{R_p}$ becomes

$$\bar{R}_p = k_p[\bar{M}]\sqrt{\frac{\phi_i \alpha I_0 [PI]_0}{k_t}}(1 - 0.25\alpha L[PI]_0 e^{\phi_i \alpha I_0 t}) e^{0.5\phi_i \alpha I_0 t} \quad (28)$$

The analytical solutions for the average monomer concentration and the average conversion ($\bar{X}$) can then be obtained by integrating eq. (28) with regard to time and using eq. (7):

$$[\bar{M}] = [M]_0 \exp\left\{2k_p\sqrt{\frac{[PI]_0}{\phi_i \alpha I_0 k_t}} \times [(1 - B/3) - (1 - Be^{\phi_i \alpha I_0 t}/3)e^{0.5\phi_i \alpha I_0 t}]\right\} \quad (29)$$

$$\bar{X} = 1 - \exp\left\{2k_p\sqrt{\frac{[PI]_0}{\phi_i \alpha I_o k_t}} \times [(1 - B/3) - (1 - Be^{\phi_i \alpha I_0 t}/3)e^{0.5\phi_i \alpha I_0 t}]\right\} \quad (30)$$

where $B = 0.25\ \alpha L[PI]_0$.

The experimental conversion data generated within this study in thin static films under a range of conditions will be compared with the model conversion predicted by eq. (30).

The following data were used in computing the theoretical conversion model:

$I_o\ (\text{mol}/(1000\ \text{scm}^2)) = I_o(\text{mW}/\text{cm}^2)/E$, where $E = h\nu N_A/\lambda$

$h = 6.626 \times 10^{-34}$ J s

$v = 3 \times 10^8$ m/s

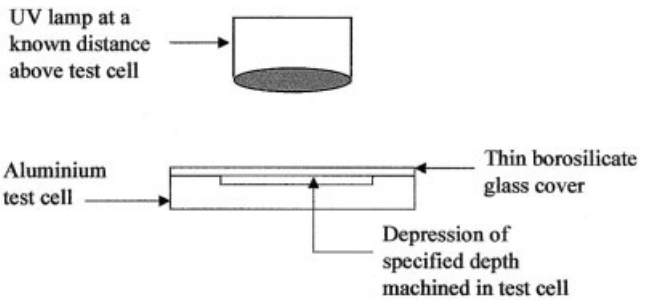

Figure 1 The setup of the static film test cell.

$N_A = 6.023 \times 10^{23}$ photons/mol
$\lambda = 366$ nm $= 366 \times 10^{-9}$ m
$\alpha_{DMPA} = 345$ L mol^{-1} cm^{-1}
[$=\varepsilon_{DMPA} \ln 10$, $\varepsilon_{DMPA} = 150$ mol L^{-1} cm^{-1} (from Goodner and Bowman[19])]
$\phi_i = 0.6$ (from Goodner and Bowman[19])
$[PI]_0 = 0.0712$ mol/L
$k_p = 16{,}300$ L mol^{-1} s^{-1} (from Beuermann et al.[20])
$k_t = 6 \times 10^7$ L mol^{-1} s^{-1} (from Beuermann et al.[20])

EXPERIMENTAL

Materials

n-Butyl acrylate (>99% purity, Aldrich) was treated with ice-cold 0.5% aqueous sodium hydroxide to remove the inhibitor, washed with water to remove the base, and left to dry overnight with anhydrous magnesium sulfate. The monomer was used directly after filtration. The DMPA (Irgacure 651) was used as received from Ciba. The solvents were pure grade and used without further treatment. Commercial oxygen-free nitrogen was used to deaerate the monomer containing the desired initiator concentration.

Apparatus and procedure

Aluminum blocks with circular depressions of accurately machined depth (Fig. 1) were used to give films with thicknesses in the range of 200–1000 μm. The monomer (50 mL) containing 2% (w/w) initiator (0.071*M*) was prepared and deaerated for at least 15 min. A small amount of the deaerated solution was pipetted in the aluminum block depression. The procedure was carried out in a nitrogen pressurized Atmos bag. A Pyrex glass plate was placed over the monomer film to remove any excess solution and to preclude oxygen when removed from the bag. Irradiation was carried out using a 1000-W flood lamp (model UV-F1000) from UV Light Technology Ltd. The lamp was enclosed in a box with the inside surfaces painted black and a front removable cover made of red acrylic to prevent any radiation escape to the surroundings when the lamp was in operation. The UV intensity was varied by changing the distance between the lamp and the test cell using a lab jack on which the aluminum block was placed. The range of UV intensities achieved was between 50 and 170 mW/cm^2 as measured by a hand held UV-A meter (model UV-M400, UV Light Technology Ltd.). A UV-light sensor was also mounted onto the edge of the lab jack and connected to a timer unit that measured the UV exposure time to 0.01 s. The effects of exposure times ranging from 10 to 40 s were studied.

Characterization

The conversion of monomer, the molecular weights, and the polydispersities were determined by gel permeation chromatography analysis using a double-column oven with 2 PLgel mixed-C type columns with a PLgel 5 μm guard operating at 30°C. Tetrahydrofuran was used as a solvent at a flow rate of 1 mL/min. The molecular weights and their distributions were calibrated against polystyrene standards. A conversion calibration was also set up using samples of monomeric and polymeric *n*-butyl acrylate.

RESULTS AND DISCUSSION

Effect of exposure time on conversion and molecular weight properties

The effect of the UV exposure time on the conversion was studied for a range of film thicknesses and UV intensities. The films were exposed to the UV beam for periods ranging from 5 to 40 s. The results for UV intensities ranging from 5 to 170 mW/cm^2 are shown in Figure 2 for a film thickness of 400 μm.

The results indicate that, at the lower UV intensities of 5, 11, and 50 mW/cm^2, the conversion increases almost linearly with the UV exposure time. At UV intensities beyond 50 mW/cm^2, the conversion increases more sharply to give conversions in excess of 50% in less than 10 s. It is also clear from the plots that higher conversion is obtained as the UV intensity is increased for any given exposure time, and conversions greater than 90% are achievable after 30 s of exposure at about 170 mW/cm^2 in the 400 μm film. Similar trends are observed for film thicknesses of 820 and 1000 μm.

We also observed that, for any given film thickness at UV intensities below 15 mW/cm^2, an induction period ranging from 2 to 10 s occurs. This induction period increases as the UV intensity is reduced. Similar induction periods have been noted for other photoinitiated systems.[10,21] The induction period in this study may be explained by radical–radical interac-

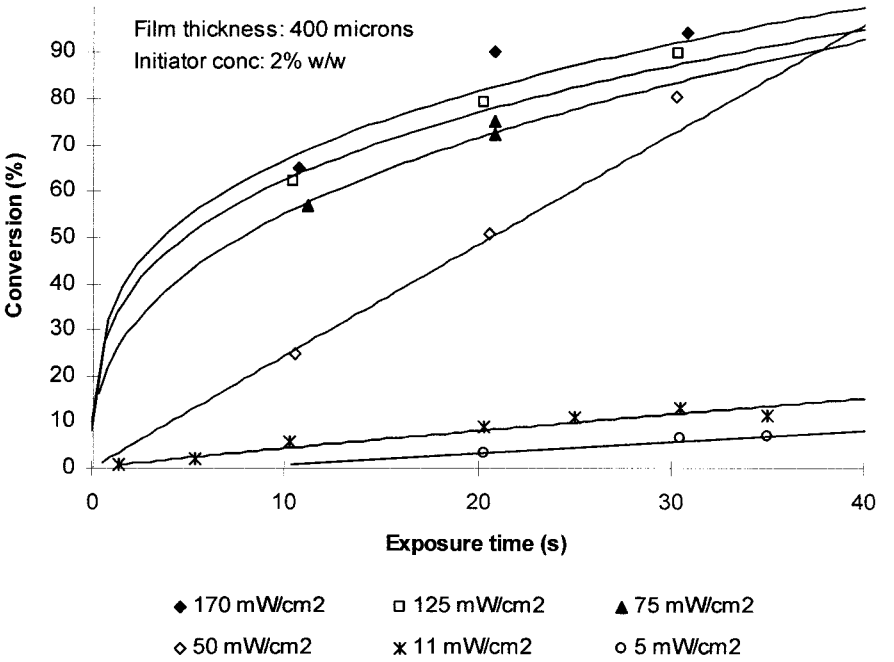

Figure 2 The effect of the UV exposure time on the conversion for a 400 μm film.

tions being favored at the lower radical concentrations achieved at lower intensities rather than radical–monomer interactions to start off active chains.[21] The inhibitory effects of oxygen[10] on the polymerization are thought to be less important here because the films are deaerated and covered to prevent atmospheric oxygen from diffusing into them. In addition, relatively thick films (200–1000 μm) are used, which would restrict any possible diffusion of oxygen to only the top layers of the static film.

The effect of the exposure time on the conversion has been theoretically modeled using eq. (30) and is shown in Figure 3. At the higher UV intensities ($\geq$50 mW/cm^2), the conversion has been modeled up to a certain UV exposure time t_{max} given by eq. (25). In the model prediction, it is assumed that the final conversion is reached at t_{max}, which corresponds to the time at which all initiator molecules have dissociated and hence polymerization stops. The model predicts that, as the intensity increases, t_{max} and the final conversion are reduced.

A comparison of Figure 2 and Figure 3 indicates that the initial experimental rates of polymerization are much slower than the initial theoretical rates for low UV intensities of 5–50 mW/cm^2. In practice, diffusion of radicals in the unagitated film may be severely restricted, an effect that is most probably further aggravated by the increasing viscosity of the medium with progress in the polymerization. By contrast, the model is based on an ideal kinetic treatment that neglects diffusion control of the polymerization steps. Furthermore, the model disregards the induction period that, in practice, retards the initial stages of the polymerization.

At higher UV intensities (125 and 170 mW/cm^2), experimental conversions as high as 90% are obtained, which are higher than the final conversion predicted by the model. This may be attributed to an increased temperature effect. It is highly likely that the large amounts of heat directed to the test sample at the much higher intensities in combination with the heat of polymerization reduce the viscosity, causing increased mobility and accessibility of the growing rad-

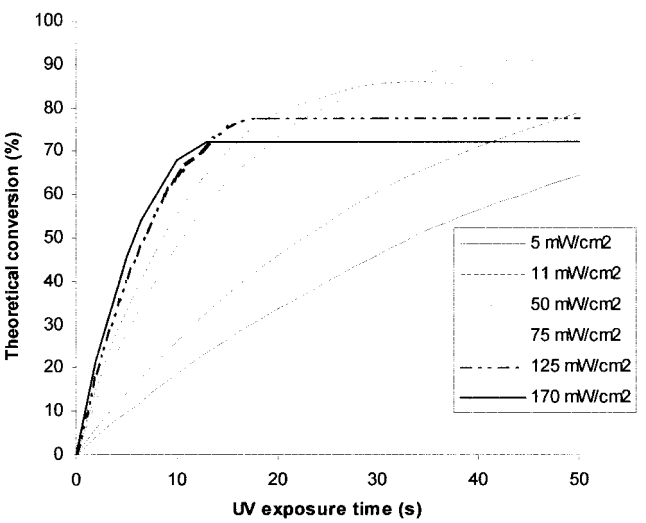

Figure 3 The effect of the UV exposure time on the theoretical conversion profiles in a 400 μm film.

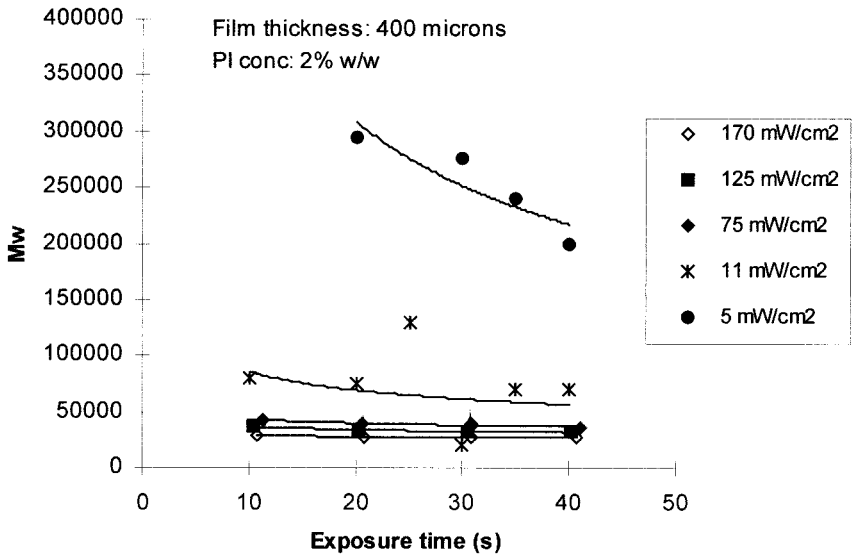

Figure 4 The effect of the exposure time on the weight-average molecular weight (M_w) in a 400 μm film at various UV intensities.

icals to monomer molecules. In a recent article Goodner and Bowman[22] modeled the influence of such temperature effects on the kinetics of photopolymerization in thick films, and our experimental observations fit with their predictions.

The typical effects of increased UV exposure time on the molecular weight properties of poly(*n*-butyl acrylate) [i.e., the weight-average (M_w) and weight-number (M_n) molecular weights and the polydispersity index (PDI)] are shown in Figures 4–6 for a film thickness of 400 μm.

Observe that the M_n and M_w tend to decrease with exposure time, the effect being more pronounced at the lowest intensity of 5 mW/cm^2, as shown in Figures 4 and 5. This reduction in molecular weights may be explained in terms of the increased number of radicals formed as more photons are absorbed over a longer duration. The presence of more primary radicals in the film is likely to encourage termination of the growing chains by the primary radicals, giving reduced molecular weights. At higher UV intensities, this reduction appears to be less important; the rise in

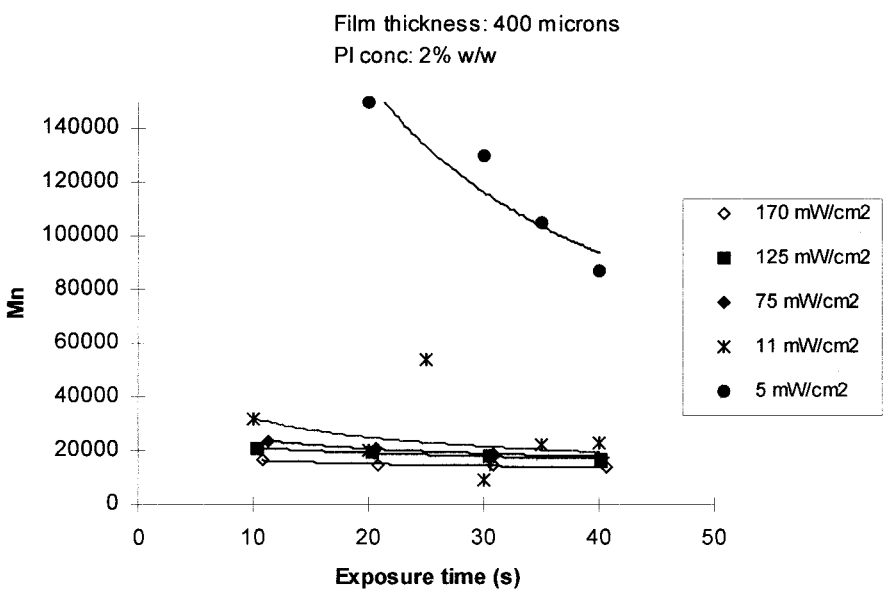

Figure 5 The effect of the exposure time on the number-average molecular weight (M_n) in a 400 μm film at various UV intensities.

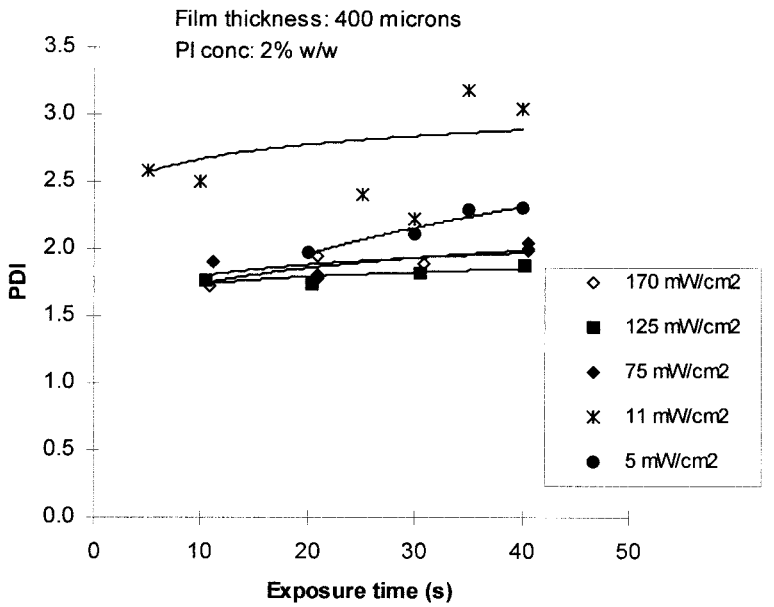

Figure 6 The effect of the exposure time on the polydispersity index (PDI) in a 400 μm film.

temperature of the sample at the high intensities promotes adiabatic conditions in the film that in turn cause the molecular weights to increase, as observed by Oster and Yang.[18] This is probably due to the increased mobility of the radical chains in the less viscous medium, thereby allowing bimolecular termination to continue taking place rather than primary termination. Thus, the molecular weights at higher intensities remain at an almost constant level because of the opposing effects.

There appears to be little change in the PDI with exposure time when high UV intensities of 75 mW/cm^2 and above are used, as seen in Figure 6. This observation is consistent with the almost constant molecular weights obtained, the reasons for which are discussed above. However, a slight increase is noticeable at 5 and 11 mW/cm^2. What is most interesting is the fact that the PDIs at 11 mW/cm^2 are much higher than those at 5 mW/cm^2, although the molecular weights follow an opposite trend. Again, this may be attributed to a larger number of radicals generated at 11 mW/cm^2, which increases the likelihood of primary radical termination and thereby broadens the molecular weight distribution. We believe that if our static film test cells had been designed to operate at isothermal conditions, we would have observed higher PDIs for the higher intensities of 75 mW/cm^2 and above that were tested in this study because the temperature effects would be eliminated.

Effect of film thickness on conversion and molecular weight properties

Film thicknesses in the range of 200 μm to 1 mm were irradiated with UV light of varying intensity to determine the effect on the conversion and molecular weight properties of polymers formed in the static film cell. We observed that a decrease in the film thickness resulted in higher conversions at any given exposure time. The typical trend is depicted in Figure 7 for a moderate UV intensity of 75 mW/cm^2. This effect was more apparent at lower exposure times.

Similar trends were obtained for 50 and 125 mW/cm^2 (Fig. 8), although the effect of the film thickness appeared to be minimized beyond an exposure time of 20 s at the higher UV intensity. There was no discernible decreasing trend with the film thickness at the lower UV intensities.

Between 50 and 125 mW/cm^2, nearly isothermal conditions can be maintained throughout the film, irrespective of the film thickness. However, UV light can penetrate thinner films more efficiently, especially in the presence of a nonphotobleaching initiator such as DMPA. At a given intensity, the average rate of radical formation is thus higher in a thinner film, allowing higher conversion to be achieved through a larger number of monomer molecules being consumed in the propagating steps. In thicker films, the effects of the spatial variation of the polymerization rates will become more significant, as has been extensively studied and discussed by Goodner and Bowman.[22] Hence, polymerization proceeds less uniformly, with the top layers achieving almost complete conversion while the bottom of the film is only partly polymerized, giving an overall lower average conversion over the thicker film.

The conversion data for tests at an even higher intensity of 170 mW/cm^2 show an opposite trend: higher conversions are obtained with thicker films

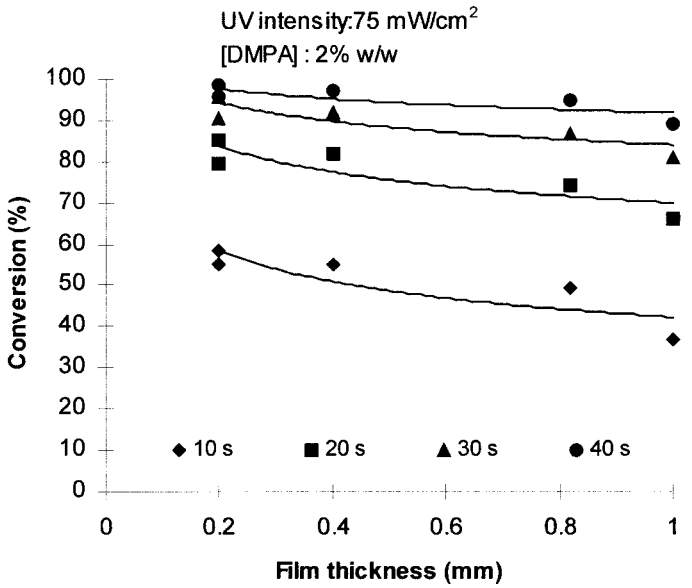

Figure 7 The effect of the film thickness at a UV intensity of 75 mW/cm^2.

rather than thinner films (Fig. 9). This could be attributable to the adiabatic conditions prevailing at this much higher intensity; the excessive heat from the lamp incident on the sample causes a larger rise in temperature in thin films than in thicker films. This would result in reduced viscosity in the thinner film, which in turn enhances the mobility of radicals and possibly the bimolecular termination process. As the active polymer chains in the thinner films come together for combination, less active chain ends become available for monomer addition. In contrast, thicker films remain relatively more viscous and therefore diffusion control limitations set in more easily, especially under gel effect conditions. Active polymer chains grow steadily by adding on more monomer molecules, causing conversion to increase. Therefore, the conversion in thin films is lower than in thicker films. Moreover, higher molecular weights and PDIs are expected in thick films at the highest UV intensities.

The theoretical effect of film thickness compares reasonably well with the observed experimental effect as shown in Figure 10, with an increase in film thickness resulting in a decrease in conversion at a moderate UV intensity of 75 mW/cm^2. Note also from Figure 10 that the experimental conversion profiles are very

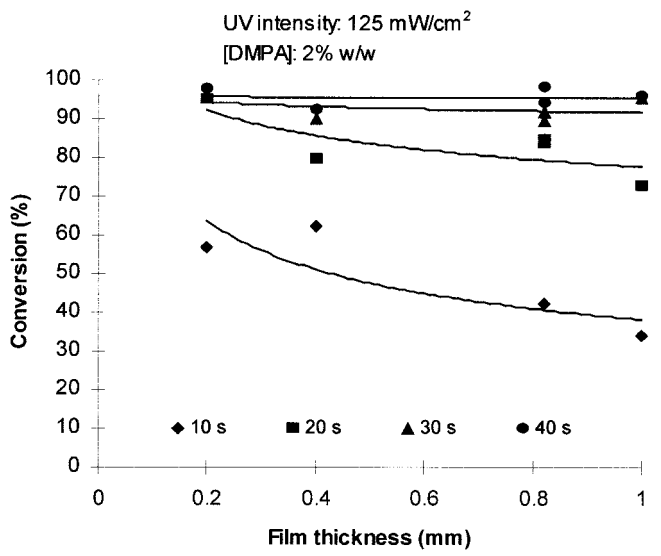

Figure 8 The effect of the film thickness on the conversion at a UV intensity of 125 mW/cm^2.

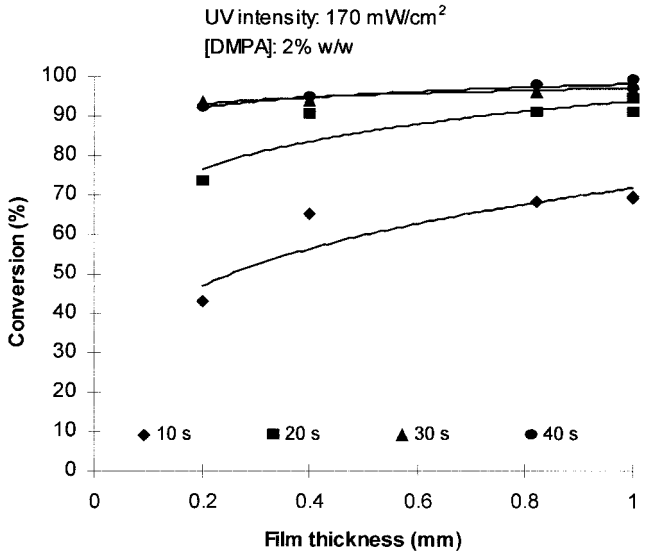

Figure 9 The effect of the thickness on conversion at a UV intensity of 170 mW/cm^2 UV.

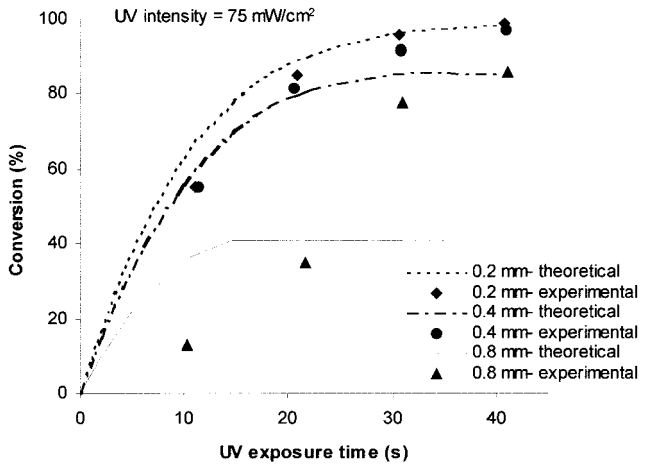

Figure 10 A comparison of the theoretical and experimental effects of the film thickness on conversion.

close to the theoretical profiles at film thicknesses of 200 and 400 μm. However, with a further increase in film thickness to 800 μm, theory predicts a lower final conversion (40%) than that obtained experimentally (>80% at 40 s). As already mentioned, the theoretical prediction is based on an ideal kinetic model that assumes polymerization stops after all initiator molecules have been used. Clearly, polymerization still continues. This may be explained by the initiator dissociation being slower because of increased attenuation of the light in the thicker film so that initiator molecules are still available over the time period of 40 s and by further addition of monomer molecules to already formed polymer chains that will necessarily be accompanied by an increase in molecular weight and PDI as polymerization progresses.

At UV intensities of $\leq$125 mW/cm^2, a decrease in film thickness is accompanied by lower M_n and M_w and lower PDI (Figs. 11–13). These trends are consistent with the effects of spatial variation in thicker films where a broader range of molecular weights would result from nonuniformity in the polymerization rates.

The trends in Figures 11–13 may be explained by considering the effect that the film thickness has on the diffusion limitations imposed on various species involved in the chain reaction steps. Diffusion of growing chains in a thinner static film is less restricted by the shorter pathlength; hence, early termination is promoted, giving lower molecular weights and less variation in the distribution of molecular weights (low PDI). As the film thickness increases, diffusion of chains becomes impeded, allowing chains to remain active longer. The chains can thus randomly grow into longer chains of varying lengths before termination eventually occurs. Although the chains are not very mobile in the viscous medium in the thick films, they are probably long enough for the radical centers to be close enough together for two of them to react and terminate by the so-called reaction diffusion process.[23,24] Thereby, the molecular weights rise and their distributions are broader.

The effects on the molecular weight properties caused by increasing the UV exposure time are also apparent here: as the UV exposure time increases, the M_n and M_w decrease for any given film thickness, the decrease in M_n being more noticeable. This observa-

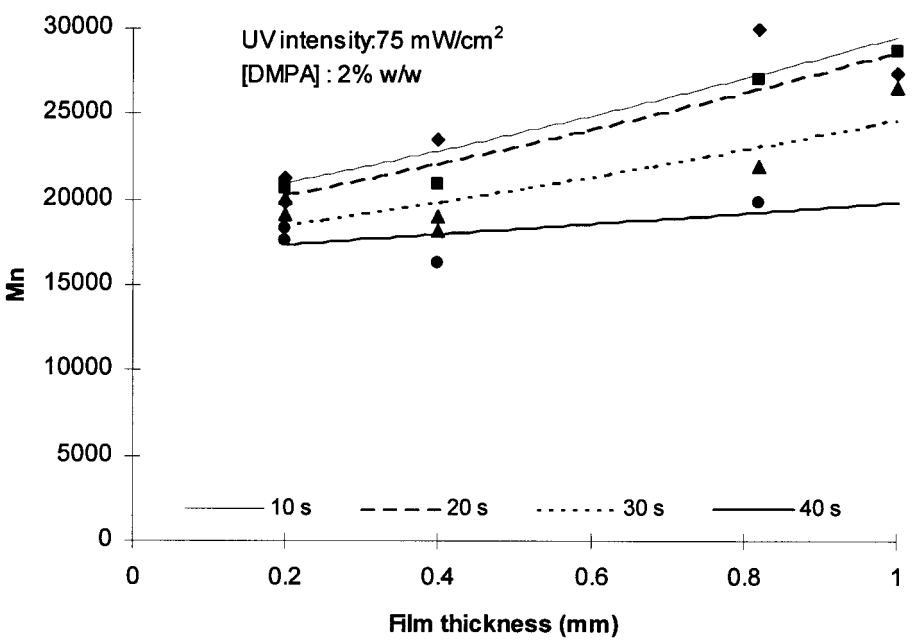

Figure 11 The effect of the film thickness on the number-average molecular weight (M_n) at a UV intensity of 75 mW/cm^2.

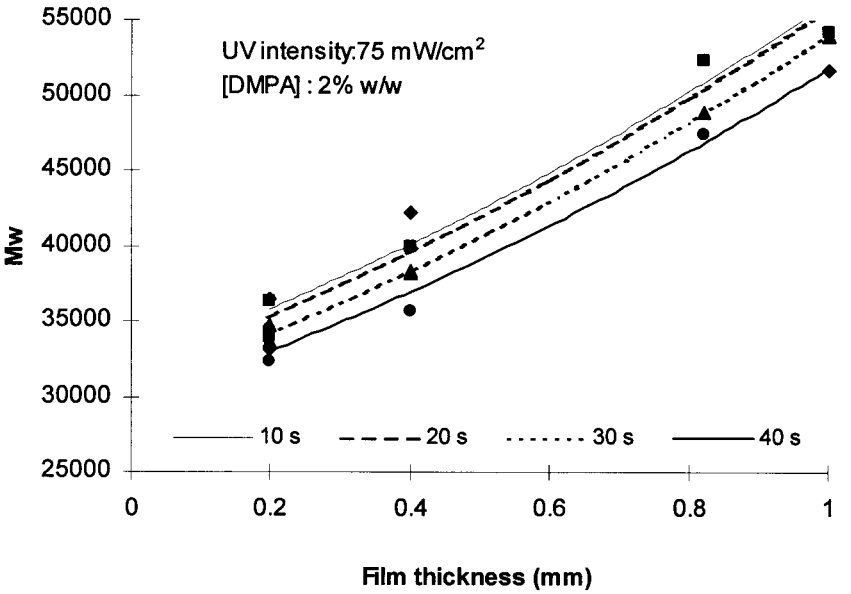

Figure 12 The effect of the film thickness on the weight-average molecular weight (M_w) at a UV intensity of 75 mW/cm^2.

tion is consistent with the profiles seen in Figures 4 and 5 and for the reasons discussed earlier in this article.

It was observed that the trends in the molecular weight properties such as those shown in Figures 11–13 were not applicable at a much higher UV intensity of 170 mW/cm^2 (Fig. 14). It would appear that the adiabatic conditions prevailing at this high UV intensity, as mentioned earlier, have a large effect on the molecular weights in the thinner films exposed to UV light for longer periods. The steady rise in temperature with exposure time in the thinner films would promote bimolecular termination, thus causing an increase in the molecular weight with exposure time in the 200 μm film, rather than a decrease.

Effect of UV intensity on polymerization kinetics and molecular weight properties

UV intensities in the 5–170 mW/cm^2 range were tested on films of varying thicknesses. In the low UV intensity range between 5 and 11 mW/cm^2, we ob-

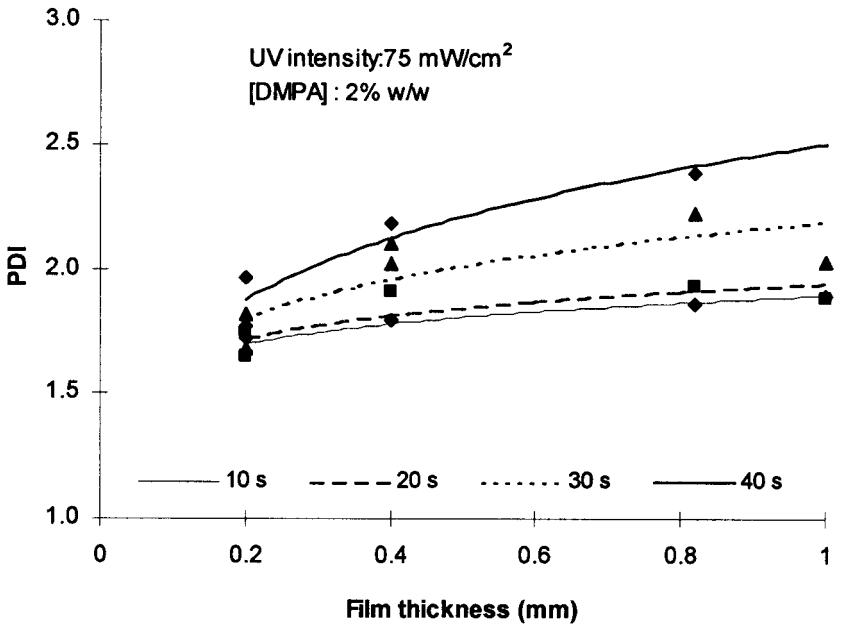

Figure 13 The effect of the film thickness on polydispersity index (PDI) of the polymer at a UV intensity of 75 mW/cm^2.

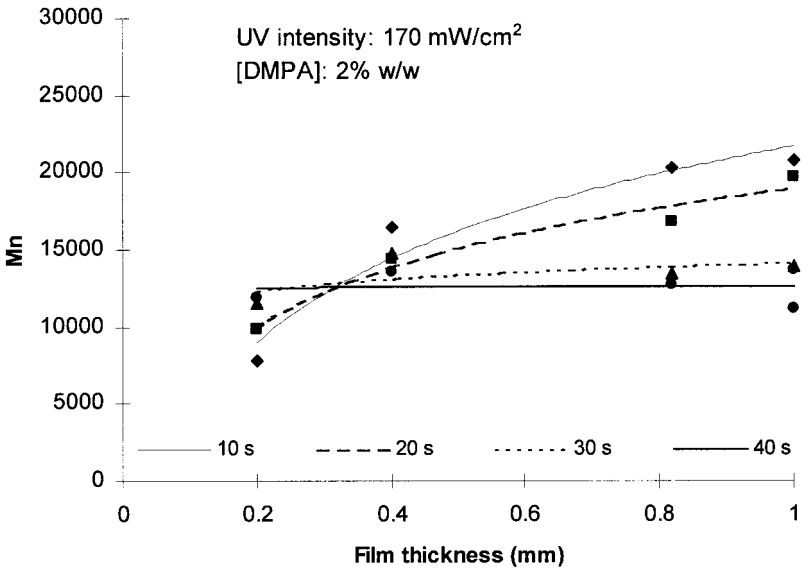

Figure 14 The effect of the film thickness on the number-average molecular weight (M_n) at a UV intensity of 170 mW/cm^2.

served that a linear relationship exists between the UV intensity and the conversions at all exposure times for all film thicknesses (Fig. 15).

In the higher UV intensity range (50–170 mW/cm^2), an optimum UV intensity is observed for all film thicknesses at which a maximum conversion is obtained (Figs. 16, 17). The optimum value appears to shift to a higher UV intensity as the film thickness increases, as seen in Figure 18.

These effects may be explained by the increased rate of initiator decomposition at higher UV intensities that results in more radicals and more polymer chains being formed. More chains consume more monomer molecules and conversion therefore rises. When the intensity rises beyond the optimum value, the number of primary radicals in the system becomes so excessive that they tend to terminate chains rather than initiate new ones. As more chains are terminated in this way, less monomer is used up and conversion therefore drops. These observations are consistent with the theoretical effects of primary radical termination on conversions achieved in photopolymerization processes, as investigated in detail by Goodner and Bowman.[19,25]

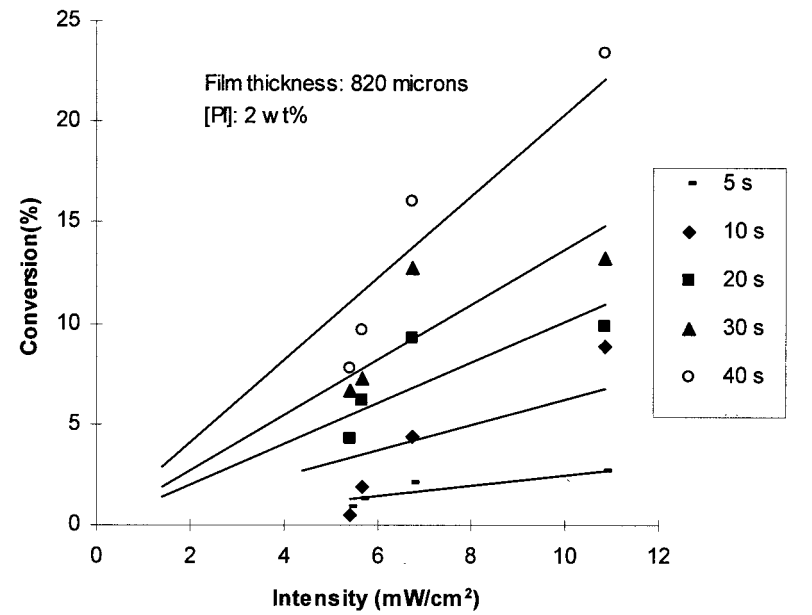

Figure 15 The effect of low UV intensities on the conversion in a 820 μm film.

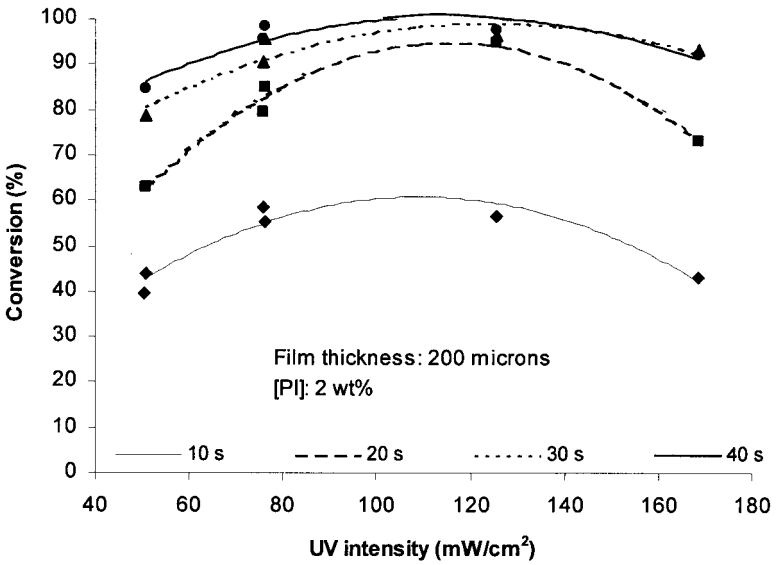

Figure 16 The effect of the moderate to high UV intensity on the conversion in a 200 μm film.

Note from Figure 18 that the optimum value shifts to a higher UV intensity as the film becomes thicker. This is because more photons need to be absorbed in a thicker film to produce primary radicals of sufficiently high concentration in order to be in excess.

A comparison of the theoretical and experimental effects of the UV intensity on the conversion in an 820 μm film is shown in Figure 19. The theoretical rate of polymerization increases with a rise in the UV intensity in the initial stages of polymerization; during this period, the theoretical rates are higher than the experimentally measured rate because of the induction period that retards the polymerization in practice. The actual conversions achieved during polymerization exceed the theoretical predictions, more so at high UV intensities and after prolonged exposure to the UV source. Increased temperature effects under these conditions would be responsible for this steady rise in conversion, as discussed earlier.

There is a decreasing trend in the molecular weight with increasing intensity for all film thicknesses over the range of UV intensities we studied (Fig. 20). There is also an increase in the PDI with increasing intensity (Fig. 21). Primary radical termination would predominate over bimolecular termination in the presence of a larger number of radicals at higher UV intensities. Hence, shorter chains are formed with a broader distribution of the molecular weights.

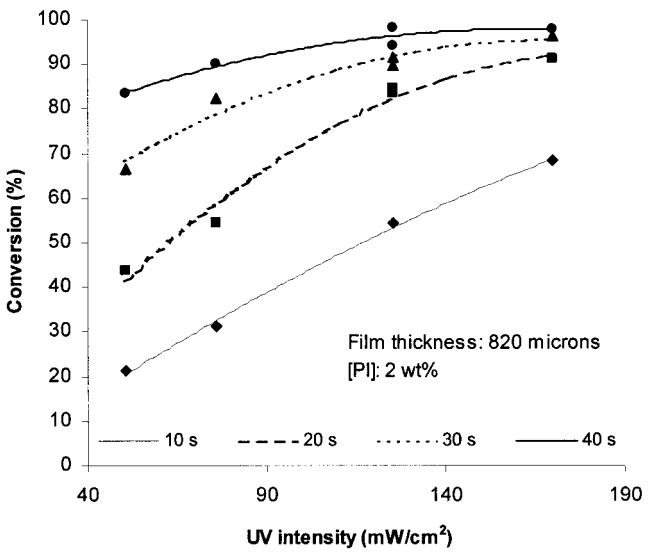

Figure 17 The effect of the moderate to high UV intensity on the conversion in a 820 μm film.

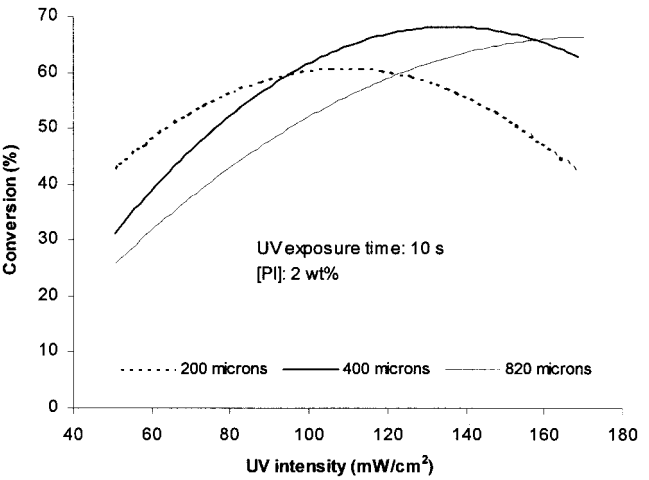

Figure 18 The effect of the film thickness on the optimum UV intensities.

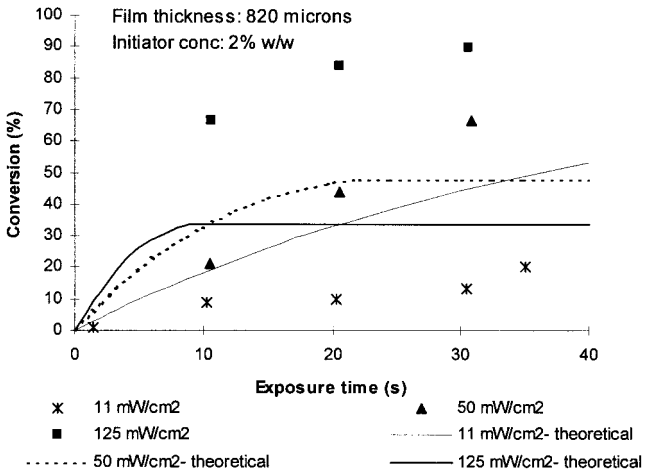

Figure 19 A comparison between the experimental and theoretical effects of the UV intensity on the conversion.

Effects of polymer glass-transition temperature

Under certain conditions of the UV intensity and film thickness, the photopolymerization of *n*-butyl acrylate progressed to a conversion of about 96% after an exposure time of 40 s (Figs. 7, 8). It is expected that complete conversion would have been achieved with longer exposure times because the glass-transition temperature (T_g) of poly(butyl acrylate) (−55°C) is well below the ambient temperature employed in this work. Vitrification effects and limiting conversions, which occur as a result of a dramatic reduction in the free volume of polymerizing systems and severe diffusion limitations,[26,27] are therefore completely avoided here. In contrast, if monomers such as methyl methacrylate or styrene, which have polymer T_g values of 105 and 100°C, respectively, were initiated at ambient temperatures under normal bulk conditions such as in a batch vessel, we would naturally expect limiting conversions well below complete conversion to be reached. However, we believe that the conditions in the thin films are rather different from those in a batch vessel. The diffusion of initiator radicals across the very short path lengths within our thin films would be less restricted, even under conditions of reduced free volume, so that the polymerization may still proceed to higher conversions in the thin film, albeit at a slower rate than that observed for a low T_g polymer. This assertion is based on the findings of Russell and coworkers[28] that, in the emulsion and suspension polymerization of methyl methacrylate at 50°C, both of which represent restricted volume systems comparable to our thin films, complete conversion was achieved in 1 day. This is a dramatic improvement in comparison to a bulk system,[29] where complete conversion was reached after 10 days at 80°C. It is interesting to note that Russell et al.[28] also criticize the free volume models for k_p in bulk systems,[30–32] suggesting instead that a significant decrease in initiator efficiencies at high conversions is responsible for the slow bulk polymerizations.

Furthermore, our results here indicate that, for those monomers with high polymer T_g, higher polymerization rates should be achieved in the static films by operating at high UV intensities (>125 mW/cm^2) over longer exposure times (>40 s) and using thicker films (>400 μm). We have shown that such a combination of operating parameters will result in nonisothermal conditions in the test cell and may cause the operating temperature to rise beyond the polymer T_g. These higher operating temperatures should eliminate vitri-

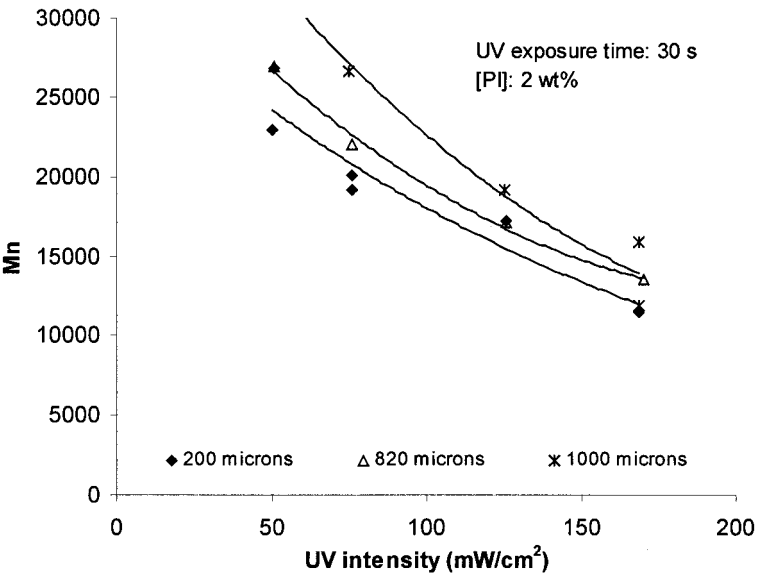

Figure 20 The effect of the UV intensity on the number-average molecular weight (M_n).

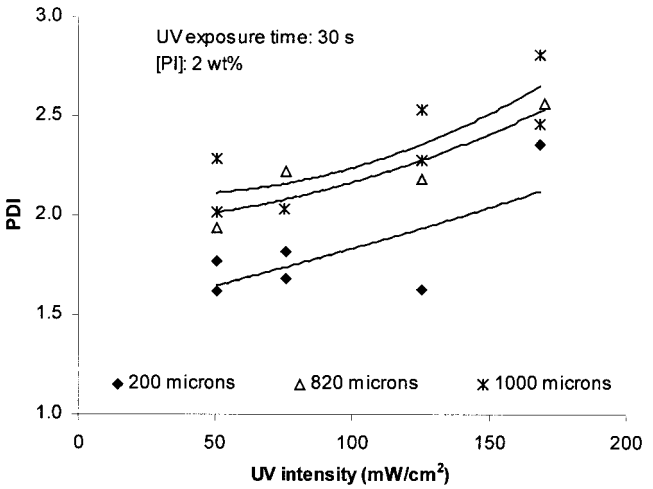

Figure 21 The effect of the UV intensity on the polydispersity index (PDI).

fication effects and thus allow the polymerization to progress to complete conversion.

Empirical data modeling

Empirical models for conversion have been generated by performing a linear regression analysis on all three physical variables under investigation (UV exposure time, UV intensity, and film thickness) in this study using the regression analysis tool in Microsoft Excel. Two models corresponding to different UV intensity ranges are presented because the polymerization clearly progresses in markedly different ways in the two ranges: low to moderate and high.

Low to moderate UV intensity range

The low to moderate UV intensity range [$5 \leq I_o$ (mW/cm^2) ≤ 50] model is obtained as

$$\text{conversion (\%)} = 0.0449t^{0.9733}I_o^{1.1422}L^{-0.04901} \qquad (R^2 = 0.934) \quad (31)$$

where t is the UV exposure time (s), I_o is the incident UV intensity (mW/cm^2), and L is the film thickness (μm). The model is applicable over the following range of variables:

$$0 \leq t \leq 40 \text{ s}$$
$$5 \leq I_o \leq 50 \text{ mW/cm}^2$$
$$200 \leq L \leq 1000 \ \mu\text{m}$$

The model in eq. (31) predicts an almost linear dependence of the conversion on each of the variables of the UV exposure time and UV intensity. However, the dependence of the conversion on the film thickness is quite weak as indicated by the low power of -0.04901. The negative power also indicates that, as the film thickness increases the conversion decreases, which is to be expected because UV penetration and therefore utilization becomes less efficient with thicker films. A reasonably good fit of the overall model to the experimental data is observed with an R^2 value of 0.934. Figure 22 shows there is generally good agreement between the predicted and actual or experimental conversions, especially when conversions do not exceed 30%.

High UV intensity range

The empirical model in the high UV intensity range [$50 < I_o$ (mW/cm^2) ≤ 170] is

$$\text{conversion (\%)} = 14.592t^{0.3667}I_o^{0.1494}L^{-0.0237} \qquad (R^2 = 0.835) \quad (32)$$

Equation (32) is applicable over the following range of variables:

$$0 \leq t \leq 40 \text{ s}$$
$$50 < I_o \leq 50 \text{ mW/cm}^2$$
$$200 \leq L \leq 1000 \ \mu\text{m}$$

It is seen from eq. (32) that, at high UV intensities, the conversion is much less dependent on both the t and I_o as indicated by the lower powers to which these variables are raised. This is most likely due to the rate of polymerization being dictated in the later stages of polymerization (i.e., at high conversions) by the chemical parameters such as the monomer and initiator concentrations and the kinetic parameters such as k_p and k_t. The dependence of the latter parameters on the

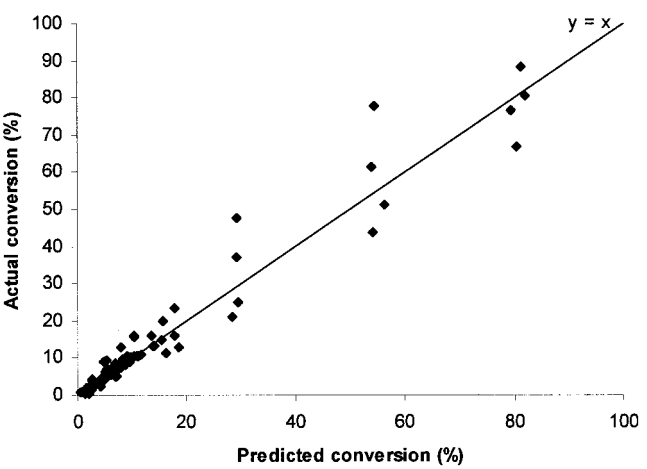

Figure 22 The experimental and predicted conversions for films of various thicknesses at low to moderate UV intensities.

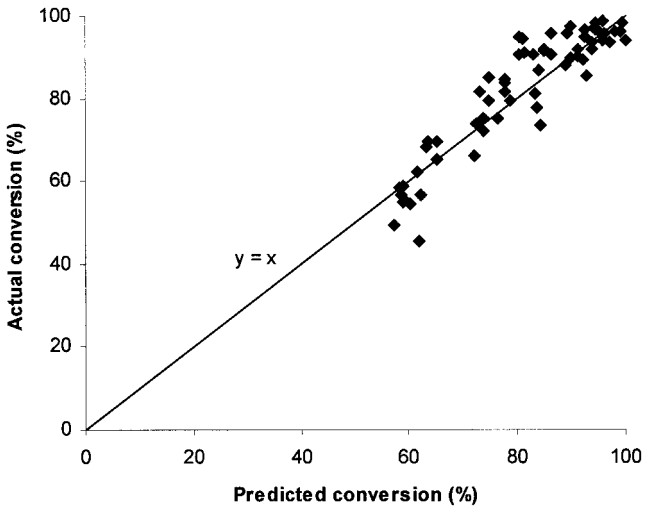

Figure 23 The experimental and predicted conversions for films of various thicknesses at high UV intensities.

viscosity of the reaction medium, which increases with conversion, would become more significant at higher conversions. Furthermore, the influence of the temperature effects on conversion would become more pronounced at higher UV intensities.

The fit of the experimental data gathered in this range of UV intensities with the empirical model in eq. (32) is shown in Figure 23. An R^2 value of 0.835 is obtained for the linear regression model in eq. (32), indicating a reasonably close fit between the experimental and model data.

CONCLUSION

The following conclusions can be drawn from this study:

1. There is a linear increase in conversion with exposure time at low to moderate UV intensities (5–50 mW/cm^2) for any film thickness, whereas conversion increases in a logarithmic manner at higher UV intensities. An induction period is evident at low UV intensities; it is reduced as the UV intensity increases. The M_n and M_w generally decrease with the exposure time, with this effect being more apparent at lower UV intensities. This is accompanied by a slight increase in the PDI with exposure time.
2. A decrease in conversion is observed in thicker films when the UV intensities do not exceed 125 mW/cm^2. However, at 170 mW/m^2, the conversion increases with the film thickness, presumably because of adiabatic conditions. There are also steady increases in the M_n, M_w, and PDI with the film thickness.
3. A linear increase in conversion with the UV intensity is obtained in a low intensity range (5–50 mW/cm^2). An optimum UV intensity is observed in the higher intensity range; the optimum value progressively increases with the film thickness from about 100 mW/cm^2 at 200 μm to 140 mW/cm^2 at 400 μm to above 180 mW/cm^2 at 820 μm.

We investigated the use of a thin film polymerization reactor based on the spinning disk reactor technology as a device capable of producing polymeric resins for industrial applications that exploit the benefits of photopolymerization. As expected, the high degree of mixing intensities achieved on the surface of a spinning disk reactor resulted in faster polymerization rates coupled with improved PDIs at higher molecular weights. A detailed investigation into the performance of the spinning disk reactor for the photopolymerization of *n*-butyl acrylate will be presented in Part II of this series.

NOMENCLATURE

A	absorbance (no units)
B	constant (no units)
C	local concentration of photoinitiator moieties (mol/L)
$\overline{C}$	layer-average concentration of photoinitiator moieties (mol/L)
E	energy/mol photons (J/mol)
h	Planck constant (J s)
I_o	incident light intensity [mol/(1000 cm^2 s) or mW/cm^2]
$\underline{I_a}$	volumetric photon absorption rate (L mol^{-1} s^{-1})
$\overline{I_a}$	average absorbed light intensity [mol/(1000 cm^2 s) or einsteins/(1000 cm^2 s)]
k_p	propagation rate constant (L mol^{-1} s^{-1})
k_t	termination rate constant (L mol^{-1} s^{-1})
k_{tc}	rate constant for termination by combination (L mol^{-1} s^{-1})
k_{td}	rate constant for termination by disproportionation (L mol^{-1} s^{-1})
l or L	pathlength or film thickness (cm)
M	monomer molecule
$M^{\cdot}$	active polymer chain
$[M]$	monomer concentration at time t (mol/L)
$[\overline{M}]_0$	layer-average monomer concentration at time t (mol/L)
$[M]_0$	initial concentration of monomer (mol/L)
N_A	Avogadro number (mol^{-1})
[PI]	average photoinitiator concentration after time t (mol/L)
$[PI]_0$	initial photoinitiator concentration (mol/L)
PDI	polydispersity index (no units)
R_i	local rate of initiation (mol L^{-1} s^{-1})

R_p local rate of propagation or rate of polymerization (mol L^{-1} s^{-1})
$\overline{R_p}$ layer-average rate of polymerization (mol L^{-1} s^{-1})
R_t local rate of termination (mol L^{-1} s^{-1})
T_g polymer glass-transition temperature (°C)
t UV exposure time (s)
t_{max} time at which all photoinitiator molecules are used up (s)
v velocity of light (m/s)
$\overline{X}$ layer-average monomer conversion at time t (%)

Greeks

α molar absorption coefficient (to base e; mol L^{-1} cm^{-1})
ϵ molar absorption coefficient (to base 10; mol L^{-1} cm^{-1})
ϕ_i quantum yield of initiation (no units)
λ wavelength of absorbed light (m)

The authors thank the Engineering and Physical Sciences Research Council (U.K.) for their financial support of this work. The first author (K.V.K.B.) thanks Dr. Guillermo Terrones, Los Alamos National Laboratory, for his useful comments on the modeling of light attenuation using nonphotobleaching initiators.

References

1. Kine, B. B.; Novak, R. W. In Concise Encyclopaedia of Polymer Science and Engineering; Kroschwitz, J. I., Ed.; Wiley: New York, 1990; p 16.
2. Sandler, J. R.; Karo, W. Polymer Syntheses, 2nd ed.; Academic: New York, 1992; Vol. 1, p 330.
3. Chem Ind (Lond) 2002, 17, 12.
4. Moad, G.; Solomon, D. H. Chemistry of Free-Radical Polymerization; Pergamon: New York, 1995; p 151.
5. Melville, H. W.; Chimayanandam, B. R. Trans Faraday Soc 1954, 50, 73.
6. Bengough, W. I.; Melville, H. W. Proc R Soc (Lond) 1954, A225, 330.
7. Roehm GmbH. Germ. Pat. DE 3,208,369, 1983.
8. Rhone-Poulenc Ind. U.S. Pat. 4,294,676, 1981.
9. Manga, J. D.; Polton, A.; Tardi, M.; Sigwalt, P. Polym Int 1998, 45, 14.
10. Decker, C.; Decker, D.; Morel, F. In Photopolymerization; Scranton, R. B., Ed.; American Chemical Society Symposium Series 673; American Chemical Society: Washington, DC, 1997.
11. Odian, G. G. Principles of Polymerization, 3rd ed.; Wiley: New York, 1991; p 222.
12. Rudin, A. Elements of Polymer Science and Engineering; Academic: New York, 1999; Chapter 6.
13. Merlin, A.; Fouassier, J. P. J Chem Phys 1981, 78, 267.
14. Terrones, G.; Pearlstein, A. J. Macromolecules 2001, 34, 3195.
15. Calvert, J. G.; Pitts, J. N. Photochemistry; Wiley: New York, 1966; p 640.
16. Lissi, E. A.; Zanoco, A. J. J Polym Sci Polym Chem Ed 1983, 21, 2197.
17. Terrones, G.; Pearlstein, A. J. Macromolecules 2001, 34, 8894.
18. Oster, G.; Yang, N.-L. Chem Rev 1968, 68, 125.
19. Goodner, M. D.; Bowman, C. N. In Solvent-Free Polymerizations and Processes. Minimization of Conventional Organic Solvents; Long, T. E., Hunt, M. O., Eds.; American Chemical Society Symposium Series 713; American Chemical Society: Washington, DC, 1998.
20. Beuermann, S.; Paquet, D. A., Jr.; McMinn, J. H.; Hutchinson, R. A. Macromolecules 1996, 29, 4206.
21. Lougnot, D. J.; Fouassier, J. P. J Polym Sci Part A: Polym Chem 1988, 26, 1021.
22. Goodner, M. D.; Bowman, C. N. Chem Eng Sci 2002, 57, 887.
23. Moad, G.; Solomon, D. H. Chemistry of Free-Radical Polymerization; Pergamon: New York, 1995; p 210.
24. O'Driscoll, K. F. In Comprehensive Polymer Science: Chain Polymerization I; Allen, G.; Berington, J. C.; Eastmond, G. C., Eds.; Pergamon: New York, 1989; Vol. 3, p 161.
25. Goodner, M. D.; Bowman, C. N. Macromolecules 1999, 32, 6552.
26. Horie, K.; Mita, I.; Kambe, H. J Polym Sci Part A-1 1968, 6, 2663.
27. Kelly, F. N.; Bueche, F. J Polym Sci 1961, 50, 549.
28. Russell, G. T.; Napper, D. H.; Gilbert, R. G. Macromolecules 1988, 21, 2141.
29. Wunderlich, W.; Stickler, M. Polym Sci Technol 1985, 31, 505.
30. Marten, F. L.; Hamielec, A. E. American Chemical Society Symposium Series 104 Polymerization reactors and processes; Henderson, J. N.; Bouton, T. C., Eds.; American Chemical Society: Washington, DC, 1979; p 43.
31. Soh, S. K.; Sundberg, D. C. J Polym Sci Polym Chem Ed 1982, 20, 1331.
32. Stickler, M. Makromol Chem 1982, 184, 2563.